



Improved illumination homogeneity increased accuracies of derived light utilization efficiency for aquatic photosynthesis-irradiance curve analysis

Qian Hu^{a,c,*}, Aiwen Zhong^a, Ian Hawes^{b,c}

^a Lushan Botanical Garden, Chinese Academy of Science, Jiujiang, China

^b Coastal Marine Field Station, University of Waikato, Tauranga, New Zealand

^c Waterways Centre for Freshwater Management, Lincoln University, Lincoln, New Zealand

ARTICLE INFO

Keywords:

Photosynthesis-irradiance curve
Improved illumination homogeneity
Light utilization efficiency
Coefficient of variations
Aquatic phototrophs

ABSTRACT

Accumulating knowledge of photo-physiological acclimation and adaptation in aquatic phototrophs to altered environmental factors are valuable for managing and conserving aquatic ecosystems. Photosynthesis-irradiance curve (PI curve) analysis is an essential technique to assess the photo-physiological states of and environmental stresses on photosystems. For PI curve analysis, replicates were rarely homogeneously illuminated, which could generate variations potentially obscuring treatment effects or lead to considerable errors. Here we present an incubation apparatus with a novel configuration of illuminating unit that supplied a gradient of irradiances with improved homogeneity. The achieved homogeneity exceeds that of other homogeneous illuminating apparatus reported for photosynthetic research. We used the elaborated apparatus to develop PI curves for *S. pectinata* photo-acclimated to contrasting light conditions in both greenhouse and field scenarios. Photo-acclimation to lower irradiances enhanced both maximum photosynthetic rates and light utilization efficiencies in general. And improved homogeneity for PI curve analysis most likely reduced variations of derived light utilization efficiency compared to those using conventional incubation apparatus. The elaborated incubation apparatus could provide insights into developments of illumination techniques for photosynthetic studies and has the potential to refine the subtleties of photo-acclimation studies.

1. Introduction

Photosynthesis is a fundamental biological process fuelling the natural world. In aquatic ecosystems, primary producers (submerged aquatic plants, macroalgae, and phytoplankton) harvest energy from the sun to support a diverse range of lives through food webs. Knowledge of photo-physiological acclimation and adaptation in aquatic phototrophs to anthropogenic activities or climate-induced environmental changes (release of new pollutants, rising temperatures, and pH, etc.) remains to be explored and could provide essential eco-physiological understandings for the management and conservation of aquatic ecosystems (Blain and Shears, 2019; Bouman et al., 2018; Cayabyab and Enriquez, 2007; Kalf, 2002; Lichtenberg and Kuhl, 2015; Pedersen et al., 2013; Piepho, 2017). Photosynthetic rates against a gradient of irradiance from darkness to beyond saturating levels form photosynthesis-irradiance (PI) curves, which assess photo-physiological states of and evaluate environmental stresses on photosystems (Delebecq et al., 2013; Hootsmans and Vermaat, 1994; Kahara and Vermaat,

2003; Phooprong et al., 2008; Schutter et al., 2012; Sorrell and Dromgoole, 1986). Rates of underwater photosynthesis are usually estimated through oxygen exchange in liquid phases. Technically, detached leaves (shoots) or algal thalli in aqueous mediums or algal cultures are incubated in sealed vials or chambers and exposed to a pre-defined gradient of irradiances. Then the amount of oxygen produced or consumed during incubations is normalized to incubation time and unit of biomass or chlorophyll-a to calculate photosynthetic rates correspondingly for the gradient of incubation irradiances to construct a PI curve.

For replications of PI curve analysis, replicates are ideally identically illuminated across a gradient of irradiances. Identical illumination can be achieved by PI curve analysis of replicates incubated in the same photo-respirational chamber under identical illumination settings, with only one PI curve analysis performed at a time, and replications require repeated analyses (Delebecq et al., 2013; Kahara and Vermaat, 2003; Shafer et al., 2011). But incubation across a gradient of irradiance levels could add up to a few hours at least, therefore repeated PI curve analyses are very time-consuming and of low efficiencies (Delebecq et al., 2013;

* Corresponding author. Lushan Botanical Garden, Chinese Academy of Science, Jiujiang, China.

E-mail address: abi10qhu@hotmail.com (Q. Hu).

<https://doi.org/10.1016/j.plaphy.2023.108027>

Received 22 January 2023; Received in revised form 29 August 2023; Accepted 7 September 2023

Available online 15 September 2023

0981-9428/© 2023 Elsevier Masson SAS. All rights reserved.

Kirsten and Peter, 1998; Masojidek et al., 2001). Alternatively, multiple PI curve analyses are usually performed simultaneously. Replicates are assumed to be illuminated under homogeneously distributed light fields across a gradient of irradiance levels, which technically has rarely been achieved in conventional incubation apparatus (Borlongan et al., 2020; Branco et al., 2017; Drew, 1979; Enriquez et al., 1995). Conventionally, frontal illuminations from various light sources (e.g. cool-white fluorescent lamps, LED panels, metal halide lamps, or halogen lamps) cast over incubation areas (Branco et al., 2017; Drew, 1979; Menendez and Sanchez, 1998; Necchi Jr and Zucchi, 2001; Sorrell et al., 2001). Regardless of the types of the light source, as light energy radiates it attenuates with increasing distance from light sources; distances to light sources vary from point to point within the illuminated incubation areas, inevitably creating a heterogeneously distributed light field over incubated samples. Unevenly distributed illumination over replicates generates variations in PI curve analysis and potentially obscures treatment effects. And heterogeneous illumination within incubation chambers was reported to generate considerable errors in PI curves analysis (Hogewoning et al., 2010). Potentially there exists a need for an incubation apparatus with homogeneous illumination over multiple replicates for PI curve analysis.

Here an elaborated incubation apparatus is presented, with its illuminating unit creatively configured to improve homogeneities for a gradient of irradiance levels. We used the elaborated incubation apparatus to develop PI curves for leaves of *Stuckenia pectinata* (a submerged angiosperm) photo-acclimated to contrasting irradiances in both greenhouse and field conditions. Subsequently, we compared variations of the derived PI curve parameters to those derived with conventional incubation apparatus.

2. Materials and methods

2.1. Elaborated incubation apparatus

The incubation apparatus consisted of an illuminating unit over a water bath for incubation (Fig. 1) and a separate sample-handling water bath. Fig. S1 (Supplementary Fig. 1) shows the apparatus in working condition, and resource availability of the key components of the apparatus is listed in Supplementary Table 1.

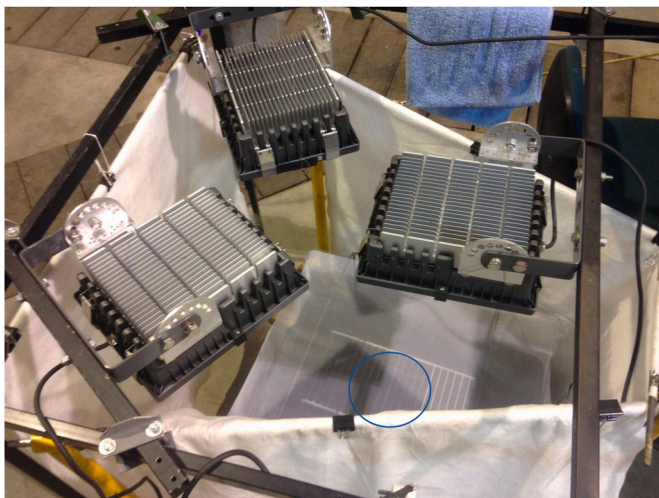


Fig. 1. Overview of the illuminating unit over an incubation water bath; the blue circle indicates the homogeneously illuminated area (the illuminating unit consists of three radially arranged LED panels over a semi-closed lightbox made of three thick layers of polypropylene fiber clothes; the incubation water bath was beneath layers of neutral density filters on a polycarbonate board).

2.1.1. Illumination unit

The illumination unit had three 100 W white LED panels fixed to a metal table frame 1.2 m above the ground (Fig. 1). The LEDs were of color temperature at 4000 k that provides a well-balanced spectral energy distribution between blue and red regions, where the respective absorption peaks of chlorophyll-a and chlorophyll-b are located, therefore were suitable for inducing photosynthesis (Specific spectral energy distribution of the LED panel is sourced from its product sheets and shown in Fig. S2). In an overhead view, the three LED lights were radially arranged with the central axis of any two LED panels forming an angle of 120° and the front of each LED panel approximately 11 cm away from the radial centre (Figs. 1 and 2B). Three thick layers of polypropylene fibre clothes (1.2 m * 1.2 m) formed (in overhead view) an equilateral triangular-shaped semi-closed lightbox (Fig. 2A) just beneath the LED lights. In the overhead view, the lightbox's triangular centre overlaps the LED lights' radical centre, and its three perpendicular bisectors overlap the LED panels' central lines (Fig. 2B). Geometrically there existed a light column along the lightbox's triangular central line with a radius of approximately 11 cm, and the total distances to the three LED light sources for any two points within any cross-section of the light column were equal, theoretically creating a homogeneous illumination over the cross-sectional area. Irradiances bounced back by the walls of the light box further enhanced the intensities of the cross-sectional areas. As a result, the illumination unit could provide a homogenous frontal illumination area (also with a radius of 11 cm) for the incubation water bath placed 0.5 m below the LED lights.

The incubation water bath's centre also overlaps the lightbox's triangular centre in the overhead view. And at just below the surface of the incubation water bath, we mapped the distribution of PAR (photosynthetic active radiation) at a resolution of 2 cm by 2 cm with a flat underwater quantum sensor (Li-192, LiCor, USA) to delineate the evenly illuminated area. To create a gradient of irradiances for PI curve analysis, different numbers of layers of white cotton fabric (as neutral density filters) were placed on an 80*80 cm polycarbonate board 10 cm above the water bath (Fig. 2A). Insertions of neutral density filters would increase scatterings of emitted photons between the LEDs and the incubation water bath, rendering the illumination more homogeneous over the incubated area. By mapping PAR distributions of the homogeneously illuminated area, we recorded the mode and range of PARs within the incubation area at each irradiance level.

2.1.2. Incubation water bath

The incubation water bath was in a black plastic tank (length 50 cm; width 30 cm; height 30 cm), equipped with a supporting rack, a submerged water pump (23w, compact pump 1001, Eheim, GmbH), an aquarium temperature-controlled heater (Thermocontrol 50, Eheim, GmbH), and a cooling unit (a temperature-controlled cooling liquid circulating water bath). The rack was 1 cm below the water surface, so the incubation vials (approximately 0.8 cm in diameter) placed on the rack were just beneath the water surface, receiving frontal illumination from LEDs above. The tank, the submerged water pump, and the aquarium heater were all in black to minimize light reflection and scatterings that generate upwelling irradiances within the water bath; the incubation area of the rack was also wrapped with black tape to minimize light reflection (Fig. S2). Because of the short light path (0.8 cm) and high transparency of the incubation medium (crystal clear), the light attenuation through the glass walls of the vials and through the incubation medium was considered ignorable, thus recorded irradiances just beneath the water surface (mentioned earlier) were used as the received irradiance by incubated leaves in vials. A submerged water pump circulated the water bath to ensure a well water-mixing regime for temperature control. The temperature could be well maintained between 5 and 35 °C with a resolution of 0.1 °C.

Three pendulums, each made of a cotton thread attached to a nail, hung from the middle of the front edge of three LEDs and dropped into the water bath. The three intersecting points at the water surface could

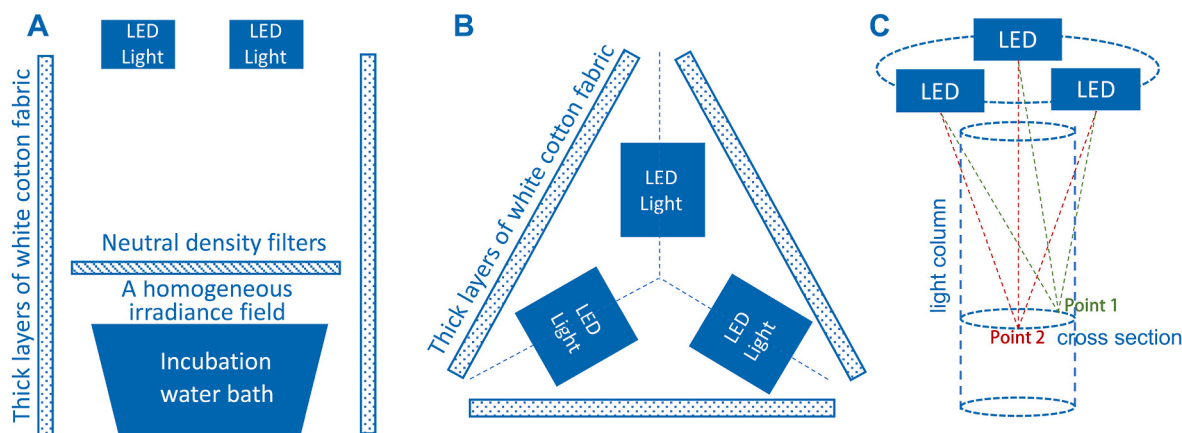


Fig. 2. Schematic representation of the side view (A) and the overhead view (B) of the configuration of an illuminating unit that delivered homogeneous illuminations over cross-sectional area of an imagined conceptual light column (C) (B: the lightbox formed an equilateral triangular; its triangular centre overlaps with the radical centre of the three LED lights, and its three perpendicular bisectors overlap with the central lines of LED lights. C: at any cross-sectional area of the imagined light column, the sum of distances to the three LED panels between any two points, the total length of green broken lines for point 1 versus that of red broken lines for point 2, are equal, so are light intensities between the two points theoretically).

indicate the location of the homogeneous-illuminated area for the position of the rack to be adjusted accordingly for incubation. Micro-oxygen sensors (PreSens GmbH, Germany) allow the choice of small incubation vials. Here glass vials (12 mL) sealed with rubber-lined screw lids were used for incubation, and up to 22 samples could be homogeneously illuminated simultaneously (Fig. S3).

2.1.3. Sample-handling water bath

The incubation water bath was exclusive for incubations. For sample preparations and dissolved oxygen (DO) sensing, there was another water bath in a plastic tank (length: 40 cm; width: 20 cm; height: 30 cm) filled with tap water of the same temperature as for incubations. The water bath had a test-tube holder to hold the incubation vials straight vertically, with its body submerged and its opening above the water surface. The sample-handling water bath was exposed to dim light at $5\text{--}10 \mu\text{mol photons m}^{-2} \text{s}^{-1}$, approximately the light compensation irradiance for leaves of submerged macrophytes. The incubation medium was prepared separately. It was enriched with sodium bicarbonate by 10 mmol/L to prevent carbon limitation and photorespiration during incubations. The medium was continuously air-bubbled, with a submerged air stone connected to an air pump, to standardize the initial oxygen content and carbon dioxide level to 100% air saturation (Madsen et al., 1993; Nielsen and Sand-Jensen, 1989).

2.2. Photosynthesis-irradiance curve analysis

Individual leaf with incubation medium was sealed in the glass vial. Together with a sample in each glass vial, there put two glass beads (5 mm in diameter). Three blank vials with only incubation mediums were prepared as controls. Incubation in darkness was created by wrapping the glass vials with aluminum foil; afterward, samples were incubated along a gradient of increasing irradiance levels step-wisely. The incubation time in darkness was 60 min and was shortened according to the irradiance levels (Table 1). Shortening incubation time at higher

irradiance levels was to prevent air saturation over 130% during incubation, above which air bubbles started to form and resulted in underestimated oxygen production. With the current experimental protocol, the oxygen saturation percentages at the end of incubations across the defined gradient of irradiance levels were in the range of 95%–124%.

Every 10 min, glass vials were tilted back and forth by hands to allow the glass beads to travel from side to side within the vial, facilitating in-vial water mixing. At the end of incubation at each irradiance level, the vials were transferred to the sample-handling water bath in dim light. Each vial was tilted back and forth again before its medium was determined for percentages of oxygen saturation, with an oxygen micro-sensor (PM-PSt7, PreSens GmbH, Germany) connected to a data logger (Microx 4, PreSens GmbH, Germany). After oxygen sensing, the incubation medium in each vial was refreshed before being transferred to the incubation apparatus at the next irradiance level.

After incubations at all light levels were complete, the oxygen evolution rates were calculated as the difference in oxygen content relative to the average of the control vials and normalized to incubation time and dry weight. When incubations began, non-linear changes in O_2 content associated with lag phases (a few minutes) of oxygen evolution of submerged leaves upon illumination after a period in darkness (Carr and Axelsson, 2008; Samuilov and Fedorenko, 1999) would occur at the lowest actinic light level, but the 60 min incubation time was long enough to render the effects of the lag phase ignorable. However, at higher actinic light levels with shortened incubation time, potential existence of a much weaker lag phase effect (Carr and Axelsson, 2008; Samuilov and Fedorenko, 1999) might just slightly under-estimate photosynthetic rates.

For each sample, oxygen evolution rates against the gradient of irradiance levels were fitted, using non-linear least square methods (the Gauss-Newton algorithm) to the hyperbolic tangent model (Eq. (1)), a robust aquatic photosynthesis-irradiance model both empirically (Jassby and Platt, 1976) and theoretically (Chalker, 1980):

$$P = P_{\text{max}} \times \tanh(\alpha \times I / P_{\text{max}}) + R \quad (\text{Equation 1})$$

Table 1

The number of filters used, the mode, range, range-to-mode ratio of distributed PAR within the incubation area, and incubation time for the eight irradiance levels.

Irradiance Levels	I	II	III	IV	V	VI	VII	VIII
Number of layers of filters	21	19	15	11	7	3	1	0
Mode of PAR ($\mu\text{mol photons m}^{-2} \text{s}^{-1}$)	20.7	46.1	65.9	89.2	129.0	191.5	242.0	317.0
Range of PAR ($\mu\text{mol photons m}^{-2} \text{s}^{-1}$)	2.6	3.6	1.8	1.8	3.0	3.0	9.0	14.0
Range/Mode ratio	12.4%	7.8%	2.7%	2.0%	2.3%	1.6%	3.7%	4.4%
Incubation time (minutes)	60	60	60	45	45	30	30	20

P is the net photosynthetic rate, and I is the photosynthetically active radiation. α is the initial slope of the curve before the onset of maximum photosynthesis and represents light utilization efficiency. P_{\max} is the light-saturated photosynthetic rate. And R is the dark respiration rate. Model fitting yields three key PI curve parameters, respectively: maximum photosynthetic rate (P_{\max}), light utilization efficiency (α), and dark respiration rate (R).

2.3. Photo-acclimations in leaves of *S. pectinata*

Photo-acclimations to contrasting light conditions were investigated for *S. pectinata* in a greenhouse and a field scenario. In greenhouse conditions, sprout tubers of *S. pectinata* were each planted in 200 mL, 8 cm tall plastic beaker filled with sediment (a mixture of fine clay and sand of equal volumes) and were placed in a glass fiber tank (diameter 2.6 m) with water depth at 0.6 m. Half of the water was replaced weekly with fresh tap water ($\text{PO}_4^{3-} = 0.1\text{--}0.13$ mg/L; $\text{NO}_3^- \text{-N} = 1.0\text{--}1.1$ mg/L). Air was bubbled continuously into the water by four air pumps (each 4 L/min, ACO-2005, HAILEA®). Water was also gently moved by three submerged pumps (23 w, 1001, EHEIM, GmbH). Throughout the experiment, the water temperature was between 15 and 20 °C, turbidity was less than 2 NTU (Nephelometric Turbidity Units), and morning pH was between 6.7 and 7.7 (PHE-7352-15 pH Sensor, Omega, US). One green polyethylene 70% shade cloth (100 cm × 60 cm) was positioned 10 cm above the water surface, creating a shaded area for low light treatment (LL). In contrast, an unshaded area in the same water body was high light treatment (HL). On sunny days, solar-noon irradiance at 25 cm deep averaged 150 $\mu\text{mol photons m}^{-2} \text{s}^{-1}$ and 520 $\mu\text{mol photons m}^{-2} \text{s}^{-1}$ for the LL and HL treatment, respectively (Li-193 Spherical Quantum Sensor and Li-1700 Data-logger Li-Cor, Inc., US). Day length through the experiment averaged 11 h. There were 16 replicates in each treatment. One month later, 8 healthy-looking fully-grown leaves from each treatment and each from a randomly selected plant were collected and analyzed for PI responses using the elaborated incubation apparatus.

In a brackish and turbid lake (Lake Ellesmere, New Zealand), a small population of *S. pectinata* persisted in a relatively sheltered bay. In March 2016, 12 surface-reaching plants in waters 0.5 m deep were randomly collected, stored in ambient water in darkness, and transferred back to the laboratory. On the sampling day, the water temperature was 25 °C, salinity was 7 ppt, and the downwelling light attenuation coefficient was 11.8 m^{-1} . The next day, 6 surface-reaching leaves and 6 leaves submerged at approximately 25 cm deep were analyzed for PI responses with the elaborated incubation apparatus. The salinity of the incubation medium was adjusted to 7 ppt with natural sea salt. An attenuation coefficient of 11.8 m^{-1} means leaves at 25 cm deep received approximately 5% of irradiance incident on surface-reaching leaves. Therefore submerged and surface-reaching leaves were considered LL acclimated and HL acclimated, respectively.

There were four light treatments (LL versus HL in the greenhouse and the field). For each replicate leaf of each treatment, photosynthetic rates were normalized to dry leaf matter (weighted after drying at 80 °C for 24 h) and fitted to the PI curve model yielding three key parameters (P_{\max} , α , R).

2.4. Effects of irradiance homogeneity on variations of P_{\max} and α

We intend to compare the efficacies in PI curve analysis between the elaborated apparatus with improved illumination homogeneity and conventional apparatus. For each of the light treatments described above, standard deviations (SD) and means were calculated for P_{\max} and α respectively, and coefficients of variation (CV) were then computed ($\text{CV} = \text{SD}/\text{mean}$) for P_{\max} and α of each light treatment to indicate efficacies of the elaborated apparatus. As for efficacies of conventional apparatus, we searched the Web of Science for studies on PI responses of

submerged macrophytes or macroalgae, analyzed with conventional incubation apparatus and through the same data processing (dry-weight standardized PI curve data fitted to the Hyperbolic Tangent model using non-linear least squares regression technique) (Jassby and Platt, 1976). PI curves of thirteen groups were sought with dry-weight standardized P_{\max} and α , both of which were reported for each group in average plus/minus either standard deviation or standard error (Branco et al., 2017; Necchi, 2004; Sorrell et al., 2001). Standard errors were converted to standard deviations (SD) if necessary ($\text{SD} = \text{SE} \times \sqrt{n}$, n is the number of replicates) before coefficients of variation (CV) were computed for each of the thirteen groups, to indicate efficacies of conventional apparatus.

The thirteen groups include apical segments of three Characeae species collected at a depth of 10 m in an ultra-oligotrophic lake (Sorrell et al., 2001), five filamentous macroalgae species each collected from a stream section (10–20 m in length) of rocky substrate and high light availability (Necchi, 2004), and five populations of submerged macrophytes (three angiosperms and two bryophytes) each from a spot in partially shaded trophic streams (Branco et al., 2017). Replicates of the apical segments of each Characeae species and of each filamentous macroalgae experienced almost identical diurnal light regime in their original habitats; while the five submerged macrophytes were pre-acclimated to a stable light regime ($140 \pm 15 \mu\text{mol photons m}^{-2} \text{s}^{-1}$, 12 h:12 h day-night cycle) at 20 °C for three days before analysis (Branco et al., 2017). Replicates of each group experienced a same light history before PI curve analysis with conventional apparatus, as were replicates of each of the four light treatments analyzed with the elaborated apparatus. Thus, photo-physiological states for replicates of each group were similar before analysis and previous plant growth conditions are thought not to contribute differently to the variations of P_{\max} and α of each group analyzed with either conventional apparatus or the elaborated one. And PI curve analysis with both conventional and elaborated apparatus involved enrichments of incubation mediums with bicarbonate, to prevent insufficient carbon supplies and photo-respirations during incubations that potentially introduce extra variations to the derived P_{\max} and α of each group. In addition, analytic procedures (such as oxygen sensing, dry weight determination etc.) for PI curve analysis with both conventional and elaborated apparatus are assumed to be performed with best practices and consistently among replicates, thus resulting in no extra variations. Therefore, though not in a strict reductionist mindset, comparisons of coefficients of variations of P_{\max} and α between conventional apparatus and the elaborated apparatus, after excluding contributions from plant growth conditions, inorganic carbon supplies, and analytic procedures as previously described, most likely could differentiate efficacies in PI curve analysis between conventional illumination homogeneities and the improved irradiance homogeneity.

2.5. Statistics

For comparison of the photo-acclimations to contrasting irradiance levels under each scenario (greenhouse and field), differences of key PI curve parameters (P_{\max} , α , and R) between LL and HL treatments were analyzed with student t-test after normality of each light group was confirmed with Shapiro-Wilk test. For efficacies between levels of illumination homogeneity, differences in CVs of P_{\max} and α were analyzed with Wilcoxon tests between the four light treatments (improved illumination homogeneity) and the thirteen groups of macroalgae and submerged macrophytes (conventional illumination homogeneity). Also, the CVs of P_{\max} and α were displayed in box plots between the two different homogeneity levels. The statistically significant level was set at 0.05. All analyses were performed in JMP statistic software (Version 13, SAS Institute Inc. USA).

3. Results

3.1. Achieved homogeneous illumination

At the incubation water bath's surface, a 415 cm² flat, circular area (23 cm in diameter) was almost homogeneously illuminated (Fig. 1 and Table 1). The elaborated incubation apparatus could provide an eight-irradiance-level gradient ranging from 21 to 317 $\mu\text{mol photons m}^{-2} \text{s}^{-1}$. The best homogeneity achieved within the incubation area, as indicated by the Range/Mode ratio, was at intermediate irradiance levels (III, IV, V, VI) where Range/Mode ratios were less than 3% (Table 1). At lower irradiance levels (I, II), the homogeneity decreased with Range/Mode ratio rising to 12.4% and 7.8% because of lower irradiance intensities (Mode). And at high irradiance levels (VII, VIII), the homogeneity also decreased slightly, with Range/Mode ratios increasing to 3.7% and 4.4% due to larger variations of irradiance (Range) (Table 1).

3.2. Photo-acclimations in leaves of *S. pectinata*

LL acclimated leaves had higher P_{max} and α , and similar R than HL acclimated leaves in both scenarios (Fig. 3). In the greenhouse, P_{max} of LL acclimated leaves ($9.16 \pm 1.74 \mu\text{g O}_2 \text{g}^{-1} \text{DW s}^{-1}$, mean \pm SD) was significantly greater than that of HL acclimated ones ($7.25 \pm 0.76 \mu\text{g O}_2 \text{g}^{-1} \text{DW s}^{-1}$) (t -test, $p < 0.01$). α of LL leaves ($0.064 \pm 0.005 \mu\text{g O}_2 \text{m}^{-2} \text{g}^{-1} \mu\text{mol}^{-1}$), although not statistically, was considered biologically larger than that of HL leaves ($0.058 \pm 0.010 \mu\text{g O}_2 \text{m}^{-2} \text{g}^{-1} \mu\text{mol}^{-1}$) (t -test, $p = 0.08$). R of LL leaves ($-0.22 \pm 0.36 \mu\text{g O}_2 \text{g}^{-1} \text{s}^{-1}$) was not different from that of HL leaves ($-0.33 \pm 0.11 \mu\text{g O}_2 \text{g}^{-1} \text{s}^{-1}$) (t -test, $p = 0.2$). In the field, P_{max} of LL leaves ($4.94 \pm 0.42 \mu\text{g O}_2 \text{g}^{-1} \text{DW s}^{-1}$) was significantly larger than that of HL leaves ($3.97 \pm 0.56 \mu\text{g O}_2 \text{g}^{-1} \text{DW s}^{-1}$) (t -test, $p < 0.01$), α of LL leaves ($0.043 \pm 0.006 \mu\text{g O}_2 \text{m}^{-2} \text{g}^{-1} \mu\text{mol}^{-1}$) was also significantly higher than that of HL leaves ($0.023 \pm 0.002 \mu\text{g O}_2 \text{m}^{-2} \text{g}^{-1} \mu\text{mol}^{-1}$) (t -test, $p < 0.01$), whereas R of LL leaves ($-0.40 \pm 0.09 \mu\text{g O}_2 \text{g}^{-1} \text{DW s}^{-1}$) was not different from that of HL leaves ($-0.37 \pm 0.09 \mu\text{g O}_2 \text{g}^{-1} \text{DW s}^{-1}$) (t -test, $p = 0.25$).

3.3. Efficacies of improved homogeneous illumination for PI curve analysis

PI curves of various submerged macrophytes and macroalgae or the same species in different light treatments analyzed with the elaborated incubation apparatus and conventional ones were compiled in Table 2. And the coefficient of variations (CV) for key PI curve parameters (P_{max} and α) of those PI curves of each group are listed in Table 3. Compared to conventional apparatus, the elaborated apparatus with improved illumination homogeneity significantly reduced variations of α , but not variations of P_{max} . The interquartile ranges of CV for P_{max} and α were respectively 9–18% and 8–16% for the group of the elaborated

apparatus with improved illumination homogeneity, and 13–24% and 17–48% for the group of conventional apparatus. CVs of the elaborated apparatus with improved illumination homogeneity were not different from those of the conventional ones for P_{max} (Wilcoxon test, $p = 0.18$) (Fig. 4A) but were significantly reduced for α (Wilcoxon test, $p = 0.03$) (Fig. 4B).

4. Discussion

This study presents an elaborated incubation apparatus with a novel configuration of illuminating unit that supplied a gradient of irradiances with elevated homogeneity for aquatic PI curve analysis. Subsequently, it demonstrates the effects of higher illumination homogeneity on variations of derived PI curve parameters (P_{max} and α). At last, notices on usages of the apparatus and its potential implications are discussed.

4.1. Achieved irradiance homogeneity

The novel configuration of three LED lights over an equilateral-triangular-shaped lightbox (Fig. 2) created a nearly homogeneously illuminated incubation area (Table 1). The homogeneity achieved in our apparatus is higher than in other reported homogeneous illuminating apparatuses for photosynthetic research (Thestrup et al., 2008; Yano and Fujiwara, 2012). For instance, Thestrup et al. (2008) presented a high-power LED homogeneous illumination platform capable of illuminating a 600 cm² flat area (20 cm by 30 cm) at 299 $\mu\text{mol photons m}^{-2} \text{s}^{-1}$ with a Range/Mean ratio of 20%. In comparison, our apparatus achieved a Range/Mode ratio of 4.4% at the highest irradiance of 317 $\mu\text{mol photons m}^{-2} \text{s}^{-1}$ for a flat area of 415 cm² (Table 1), a better homogeneity at a higher irradiance than the homogeneous illumination platform in Thestrup et al. (2008). Again, Yano and Fujiwara (2012) reported a plant lighting system that could illuminate an area of 1800 cm² uniformly at 438 $\mu\text{mol photons m}^{-2} \text{s}^{-1}$ with a coefficient of variation of 9.6%. In comparison, our apparatus, although casting a lower irradiance (317 $\mu\text{mol photons m}^{-2} \text{s}^{-1}$) over a smaller area (415 cm²), created a much higher homogeneity with a Range/Mode at 4.4% (it is worth noting variations computed by Range/Mode are larger than by coefficients of variation that is SD/Mean). Potentially our illuminating unit could be constructed at a larger size while retaining its configuration to achieve a greater illuminated area and, be equipped with more powerful LED panels to obtain higher irradiances. The configuration of our illuminating unit may provide technical insights for achieving a homogeneous frontal illumination over a large and flat area.

4.2. Improved irradiance homogeneity for photosynthesis research

The elaborated incubation apparatus successfully developed photosynthesis-response curves for *S. pectinata* in four light treatments under two scenarios (Fig. 3). Acclimations to lower irradiance levels

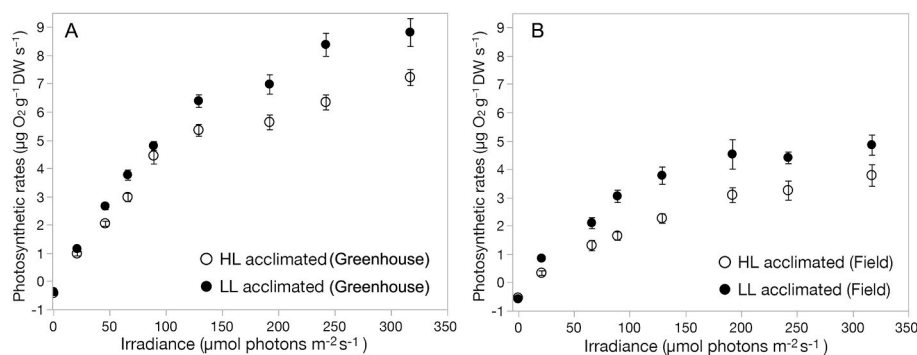


Fig. 3. Photosynthetic rates against irradiance for HL acclimated and LL acclimated leaves of *S. pectinata* in the greenhouse (A) and in field (B) scenarios (error bars represent standard error of the mean).

Table 2

Compiled list of taxonomy, P_{\max} , α , number of replicates analyzed, and original data sources for reported PI curves developed with the elaborated incubation apparatus and conventional ones (P_{\max} and α are presented in mean \pm standard deviation).

	Taxonomy	P_{\max}	α	Number of replicates	Data source
<i>S. pectinata</i> (HL-Greenhouse)	Angiosperm	7.25 \pm 0.76 ($\mu\text{g O}_2 \text{ g}^{-1} \text{ DW s}^{-1}$)	0.058 \pm 0.010 ($\mu\text{g O}_2 \text{ m}^2 \text{ g}^{-1} \text{ DW } \mu\text{mol}^{-1}$ photons)	8	this study
<i>S. pectinata</i> (LL-Greenhouse)	Angiosperm	9.16 \pm 1.74 ($\mu\text{g O}_2 \text{ g}^{-1} \text{ DW s}^{-1}$)	0.064 \pm 0.005 ($\mu\text{g O}_2 \text{ m}^2 \text{ g}^{-1} \text{ DW } \mu\text{mol}^{-1}$ photons)	8	this study
<i>S. pectinata</i> (HL-Field)	Angiosperm	3.97 \pm 0.56 ($\mu\text{g O}_2 \text{ g}^{-1} \text{ DW s}^{-1}$)	0.023 \pm 0.002 ($\mu\text{g O}_2 \text{ m}^2 \text{ g}^{-1} \text{ DW } \mu\text{mol}^{-1}$ photons)	5	this study
<i>S. pectinata</i> (LL-Field)	Angiosperm	4.94 \pm 0.42 ($\mu\text{g O}_2 \text{ g}^{-1} \text{ DW s}^{-1}$)	0.043 \pm 0.006 ($\mu\text{g O}_2 \text{ m}^2 \text{ g}^{-1} \text{ DW } \mu\text{mol}^{-1}$ photons)	5	this study
<i>Chara fibosa</i>	Characeae	35.0 \pm 5.2 ($\mu\text{mol C g}^{-1} \text{ DW h}^{-1}$)	1.5 \pm 0.6 ($\mu\text{mol C g}^{-1} \text{ h}^{-1}$)/($\mu\text{mol m}^{-2} \text{ s}^{-1}$)	4	Sorrell et al. (2001)
<i>Chara globularis</i>	Characeae	55.0 \pm 9.6 ($\mu\text{mol C g}^{-1} \text{ DW h}^{-1}$)	2.3 \pm 1.0 ($\mu\text{mol C g}^{-1} \text{ h}^{-1}$)/($\mu\text{mol m}^{-2} \text{ s}^{-1}$)	4	Sorrell et al. (2001)
<i>Chara corallina</i>	Characeae	61.9 \pm 10.8 ($\mu\text{mol C g}^{-1} \text{ DW h}^{-1}$)	2.8 \pm 1.0 ($\mu\text{mol C g}^{-1} \text{ h}^{-1}$)/($\mu\text{mol m}^{-2} \text{ s}^{-1}$)	4	Sorrell et al. (2001)
<i>Cladophora glomerata</i>	Filamentous Green Algae	5.3 \pm 0.6 ($\text{mg O}_2 \text{ g}^{-1} \text{ DW h}^{-1}$)	0.02 \pm 0.01 ($\text{mg O}_2 \text{ g}^{-1} \text{ DW h}^{-1}$)/($\mu\text{mol m}^{-2} \text{ s}^{-1}$)	5	Necchi (2004)
<i>Nitella furcata</i> var. <i>sieberi</i>	Filamentous Green Algae	35.5 \pm 1.5 ($\text{mg O}_2 \text{ g}^{-1} \text{ DW h}^{-1}$)	0.10 \pm 0.01 ($\text{mg O}_2 \text{ g}^{-1} \text{ DW h}^{-1}$)/($\mu\text{mol m}^{-2} \text{ s}^{-1}$)	5	Necchi (2004)
<i>Rhizoclonium hieroglyphicum</i>	Filamentous Green Algae	6.4 \pm 0.7 ($\text{mg O}_2 \text{ g}^{-1} \text{ DW h}^{-1}$)	0.02 \pm 0.01 ($\text{mg O}_2 \text{ g}^{-1} \text{ DW h}^{-1}$)/($\mu\text{mol m}^{-2} \text{ s}^{-1}$)	5	Necchi (2004)
<i>Spirogyra</i> sp.	Filamentous Green Algae	31.2 \pm 3.9 ($\text{mg O}_2 \text{ g}^{-1} \text{ DW h}^{-1}$)	0.02 \pm 0.01 ($\text{mg O}_2 \text{ g}^{-1} \text{ DW h}^{-1}$)/($\mu\text{mol m}^{-2} \text{ s}^{-1}$)	5	Necchi (2004)
<i>Compsopogon coeruleus</i>	Filamentous Red Algae	4.8 \pm 0.8 ($\text{mg O}_2 \text{ g}^{-1} \text{ DW h}^{-1}$)	0.12 \pm 0.04 ($\text{mg O}_2 \text{ g}^{-1} \text{ DW h}^{-1}$)/($\mu\text{mol m}^{-2} \text{ s}^{-1}$)	5	Necchi (2004)
<i>Apinagia reidellii</i>	Angiosperm	2.4 \pm 0.5 ($\text{mg O}_2 \text{ g}^{-1} \text{ DW h}^{-1}$)	0.09 \pm 0.01 ($\text{mg O}_2 \text{ g}^{-1} \text{ DW h}^{-1}$)/($\mu\text{mol m}^{-2} \text{ s}^{-1}$)	5	Branco et al. (2017)
<i>Egeria densa</i>	Angiosperm	4.2 \pm 2.8 ($\text{mg O}_2 \text{ g}^{-1} \text{ DW h}^{-1}$)	0.06 \pm 0.03 ($\text{mg O}_2 \text{ g}^{-1} \text{ DW h}^{-1}$)/($\mu\text{mol m}^{-2} \text{ s}^{-1}$)	5	Branco et al. (2017)
<i>Utricularia</i> sp.	Angiosperms	11.0 \pm 2.8 ($\text{mg O}_2 \text{ g}^{-1} \text{ DW h}^{-1}$)	0.17 \pm 0.02 ($\text{mg O}_2 \text{ g}^{-1} \text{ DW h}^{-1}$)/($\mu\text{mol m}^{-2} \text{ s}^{-1}$)	5	Branco et al. (2017)
<i>Thamniopsis pendula</i>	Bryophytes	2.4 \pm 0.9 ($\text{mg O}_2 \text{ g}^{-1} \text{ DW h}^{-1}$)	0.11 \pm 0.04 ($\text{mg O}_2 \text{ g}^{-1} \text{ DW h}^{-1}$)/($\mu\text{mol m}^{-2} \text{ s}^{-1}$)	5	Branco et al. (2017)
<i>Fissidens</i> sp.	Bryophytes	1.4 \pm 0.2 ($\text{mg O}_2 \text{ g}^{-1} \text{ DW h}^{-1}$)	0.14 \pm 0.05 ($\text{mg O}_2 \text{ g}^{-1} \text{ DW h}^{-1}$)/($\mu\text{mol m}^{-2} \text{ s}^{-1}$)	5	Branco et al. (2017)

Table 3

Coefficients of variation for P_{\max} and α for the submerged macrophytes or macroalgae listed in Table 2 analyzed under illuminations of improved versus conventional homogeneity levels.

Species	P_{\max}	α	Illumination Homogeneity
<i>S. pectinata</i> (HL greenhouse)	10.5%	17.2%	Improved
<i>S. pectinata</i> (LL greenhouse)	19.0%	7.8%	Improved
<i>S. pectinata</i> (HL field)	14.1%	8.7%	Improved
<i>S. pectinata</i> (LL field)	8.5%	14.0%	Improved
<i>Chara fibosa</i>	14.8%	40.0%	Conventional
<i>Chara globularis</i>	17.4%	43.4%	Conventional
<i>Chara corallina</i>	17.4%	35.6%	Conventional
<i>Cladophora glomerata</i>	11.3%	50%	Conventional
<i>Nitella furcata</i> var. <i>sieberi</i>	4.2%	10.0%	Conventional
<i>Spirogyra</i> sp.	12.5%	50%	Conventional
<i>Compsopogon coeruleus</i>	16.7%	33.0%	Conventional
<i>Cladophora glomerata</i>	11.3%	50%	Conventional
<i>Apinagia reidellii</i>	20.8%	11.1%	Conventional
<i>Egeria densa</i>	66.7%	50%	Conventional
<i>Utricularia</i> sp.	25.5%	11.8%	Conventional
<i>Thamniopsis pendula</i>	37.5%	36.4%	Conventional
<i>Fissidens</i> sp.	14.3%	35.7%	Conventional

involved higher maximum photosynthetic rates and boosted light utilization efficiencies, compatible with strategies of low-light acclimations in algae and submerged macrophytes in general (Anderson et al., 1995; Moejes et al., 2017; Walters, 2005).

Homogeneous illumination over a large flat area is difficult to achieve (Chertov et al., 2012). Conventional incubation apparatus did not pay extra attention to improving the homogeneity of distributed irradiance for PI curve analysis, likely because their illumination homogeneity was sufficient for addressing the scientific inquiries on

photo-physiologies (Drew, 1977; Necchi Jr and Zucchi, 2001; Pilon and Santamaria, 2002; Sorrell et al., 2001; Titus and Adams, 1979). Only Hogewoning et al. (2010) reported heterogeneous irradiance within incubation chambers led to considerable errors in PI curves analysis, serious underestimation of light utilization efficiencies and urged the development of homogeneous illuminations. In this study, we found that improved homogeneity of illumination likely reduced variations in derived light utilization efficiency (α) but not in maximum photosynthetic rate (P_{\max}) (Fig. 4). Reduced variations in α of the improved irradiance homogeneity group were for leaves of *S. pectinata* (submerged angiosperm), when compared to those of the conventional illumination homogeneity group for photosynthetic tissues of a wide range of macroalgae and submerged macrophytes (Table 2). The cellular arrangement in leaves of *S. pectinata*, an angiosperm, is expected to be more complicated than that in photosynthetic tissues of macroalgae (filamentous algae and Characeae species) and of bryophytes, which comprise the majority (10 out of 13) of species of the conventional illumination homogeneity group (Table 2). Simpler cellular arrangements logically result in more evenly distributed irradiance and smaller variations in photo-physiological states among photosystems within photosynthetic tissues, therefore, smaller variations of α . Then variations of α were expected to be larger for *S. pectinata* (improved homogeneity group) than for macroalgae and bryophytes (conventional homogeneity group) had variations of α been attributed to intrinsic structural differences of photosynthetic tissues among species. Thus, most likely reductions in the variation of α are attributed to improved homogeneity of irradiances. Improved homogeneity did not significantly affect variations in P_{\max} , likely because P_{\max} is light-saturated, where photon absorption rates exceed steady-state electron transport from water to CO_2 (Falkowski and Raven, 2007b), and is less sensitive to variations of incident irradiances.

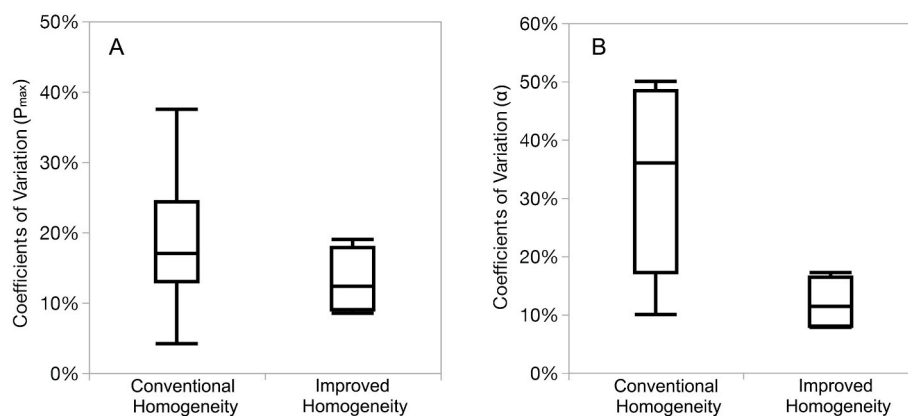


Fig. 4. Boxplots of coefficients of variation for P_{max} (A) and α (B) of PI curves developed under illuminations of conventional versus improved homogeneity.

More accurate estimation of light utilization efficiency (α) of submerged macrophytes (and potentially phytoplankton) benefits sophisticated photo-physiological research. As α is related to the relative size (functional cross-section of photosystem II) and the numbers of photosynthetic units (Falkowski and Raven, 2007a), increased accuracy could potentially indicate fine-tunings of photosynthetic apparatus that is too subtle to be revealed. Photo-acclimations in aquatic phototrophs to variable light intensities are well understood (Anderson et al., 1995; Huner et al., 2012; Walters, 2005), but their acclimation strategies to changes in underwater spectrum or waters of different optic properties are relatively less explored. Improved accuracy in α may reveal subtle effects of slightly different spectral quality on photon absorption rates for phytoplankton and submerged macrophytes. The illuminating unit of the apparatus could be further adapted for studies on photosynthetic efficiencies associated with secondary pigment synthesis in responses to different spectral qualities (Borlongan et al., 2020). Due to rapid developments in LED illuminating technology, irradiances of self-defined spectrum distribution (including monochromes) could be modulated (Glemser et al., 2016; Yano and Fujiwara, 2012) such that the LED panels in our apparatus could be replaced with ones in concordance with defined experimental spectrums, to develop spectrum-specific PI curves.

4.3. Notices on and implications of the incubation apparatus

The novelty of the reported incubation apparatus lies in the geometry of its illuminating unit, which has, compared to many conventional apparatuses, improved homogeneities of frontal illuminations over a circular area for incubations (Fig. 2). Although we only reported homogeneous illumination at the water surface of the incubation water bath, theoretically the illuminating unit should have created homogeneous illuminations at any depth through the water bath. Because for any cross section of the imagined light column, total distances to the three LEDs were the same for any two points within the cross-sectional area, the very rationale behind the homogeneous illumination (Fig. 2C). Ideally, incubation vials could be placed deeper in the water bath while receiving lower irradiance, which attenuates as distances (D) from the LEDs increase (and theoretically following a function that is $I_d = I_0 / (4\pi D^2)$, where I_0 and I_d are light intensity at just beneath the LEDs and at depth d in the water bath respectively). But technically, the tank walls of the water bath likely blocked scattered irradiances from the light box, reducing the irradiances in the water bath further, therefore we chose to place incubated samples just beneath the water surface. In this study, we used small-sized glass vials of short diameters (0.8 cm) filled with highly transparent incubation mediums, such that we could ignore the light attenuation through the incubation medium for convenience. However, if optically active incubation mediums (such as algal cultures) were incubated or the ratio of the vials' diameter (light path) to their distances from the light source (50 cm in our case) was not close to zero,

light attenuation through the incubation medium would need to be accounted. Either by estimations based on light attenuation coefficients of incubation mediums (determined separately) and length of the light path, or by direct in-vial measurements using miniaturized light sensors.

Besides being used in incubation apparatus for PI curve analysis, the illuminating unit could be installed in other frontal-illumination providing apparatus, such as plant growth chambers where replicate plants receive downwelling irradiance. Also, designs of photobioreactors for algal culturing might benefit from the geometry of our illuminating unit. A number of bench-top experimental photobioreactors (e.g. Labfor 5 LUX, PSI Photobioreactor FMT 150, and PSI Multi-Cultivator MC 1000, as mentioned in Glemser et al. (2016)) utilize frontal illumination, however, the illuminated surface of algal cultures are likely not receiving homogeneous illumination, because the sum of distances to all the LED chips is not the same, particularly between the central area and the marginal area of illuminated areas. Our illuminating unit, if adapted appropriately, would likely render the frontal illuminations received by algal cultures more homogeneous.

5. Conclusions

This study presents an elaborated incubation apparatus that supplied a gradient of irradiance levels with improved homogeneity for aquatic photosynthesis-irradiance curve developments. The achieved homogeneity was created with a novel configuration of three LED panels over an equilateral triangular-shaped lightbox and has exceeded the homogeneities of other reported homogeneous-illuminating apparatus for photosynthetic research. The configuration of our illuminating unit may provide insights for advancing techniques in photosynthetic and botanical research that require a homogeneous frontal illumination. Improved illumination homogeneity likely increased accuracies of derived light utilization efficiency, which could potentially refine the subtleties of photo-acclimation studies.

Funding

The study is co-funded by the Waihora Ellesmere Trust (New Zealand); the Oversea Talent Fund of Jiangxi Province (20212BCJ25026); the Science Collaboration Fund of Jiangxi Province (2021BDH80012); and the Research and Development Fund of Jiangxi Province (20192BBFL60018).

Authors' contributions

QH and IH contributed to the conception and design of the method, QH contributed to the construction of the apparatus, data acquisition, and manuscript writing, and AZ provided valuable suggestions on the manuscript.

Declaration of competing interest

The authors declare that they have no known competing financial interests or personal relationships that could have appeared to influence the work reported in this paper.

Data availability

Data will be made available on request.

Acknowledgments

We thank Warwick Hill at the Waterways Centre, Lincoln University, for help with technical setup.

Appendix A. Supplementary data

Supplementary data to this article can be found online at <https://doi.org/10.1016/j.plaphy.2023.108027>.

References

- Anderson, J.M., Chow, W.S., Park, Y.I., 1995. The grand design of photosynthesis: acclimation of the photosynthetic apparatus to environmental cues. *Photosynth. Res.* 46, 129–139.
- Blain, C.O., Shears, N.T., 2019. Seasonal and spatial variation in photosynthetic response of the kelp *Ecklonia radiata* across a turbidity gradient. *Photosynth. Res.* 140, 21–38.
- Borlongan, I.A., Suzuki, S., Nishihara, G.N., Kozono, J., Terada, R., 2020. Effects of light quality and temperature on the photosynthesis and pigment content of a subtropical edible red alga *Meristotheca papulosa* (Solieriaceae, Gigartinales) from Japan. *J. Appl. Phycol.* 32, 1329–1340.
- Bouman, H.A., Platt, T., Doblin, M., Figueiras, F.G., Gudmundsson, K., Gudfinnsson, H. G., Huang, B.Q., Hickman, A., Hiscock, M., Jackson, T., Lutz, V.A., Melin, F., Rey, F., Pepin, P., Segura, V., Tilstone, G.H., van Dongen-Vogels, V., Sathyendranath, S., 2018. Photosynthesis-irradiance parameters of marine phytoplankton: synthesis of a global data set. *Earth Syst. Sci. Data* 10, 251–266.
- Branco, C.C.Z., Riolfi, T.A., Cruilhas, B.P., Tonetto, A.F., Bautista, A.I.N., Necchi, O., 2017. Tropical lotic primary producers: Who has the most efficient photosynthesis in low-order stream ecosystems? *Freshw. Biol.* 62, 1623–1636.
- Cayabyab, N.M., Enriquez, S., 2007. Leaf photoacclimatory responses of the tropical seagrass *Thalassia testudinum* under mesocosm conditions: a mechanistic scaling-up study. *New Phytol.* 176, 108–123.
- Carr, H., Axelsson, L., 2008. Photosynthetic utilization of bicarbonate in *Zostera marina* is reduced by inhibitors of mitochondrial ATPase and electron transport. *Plant Physiol.* 147, 879–885.
- Chalker, B.E., 1980. Modeling light saturation curves for photosynthesis: an exponential function. *J. Theor. Biol.* 84, 205–215.
- Chertov, A.N., Gorbunova, E.V., Korotaev, V.V., Peretyagin, V.S., Serikova, M.G., 2012. Simulation of the Multicomponent Radiation Source with the Required Irradiance and Color Distribution on the Flat Illuminated Surface. *OPTICAL MODELLING AND DESIGN II*.
- Delebecq, G., Davoult, D., Menu, D., Janquin, M.-A., Dauvin, J.-C., Gevaert, F., 2013. Influence of local environmental conditions on the seasonal acclimation process and the daily integrated production rates of *Laminaria digitata* (Phaeophyta) in the English Channel. *Mar. Biol.* 160, 503–517.
- Drew, E.A., 1977. The physiology of photosynthesis and respiration in some Antarctic marine algae. *Br. Antarct. Surv. Bull.* 46, 59–76.
- Drew, E.A., 1979. Physiological aspects of primary production in seagrasses. *Aquat. Bot.* 7, 139–150.
- Enriquez, S., Duarte, C.M., Sandjensen, K., 1995. Patterns in the photosynthetic metabolism of mediterranean macrophytes. *Mar. Ecol. Prog. Ser.* 119, 243–252.
- Falkowski, P.G., Raven, J.A., 2007a. Light absorption and energy transfer in the photosynthetic apparatus. In: Falkowski, P.G., Raven, J.A. (Eds.), *Aquatic Photosynthesis*, STU - Student Edition. Princeton University Press, pp. 44–80.
- Falkowski, P.G., Raven, J.A., 2007b. Photosynthetic electron transport and photophosphorylation. In: Falkowski, P.G., Raven, J.A. (Eds.), *Aquatic Photosynthesis*, STU - Student Edition. Princeton University Press, pp. 118–155.
- Glemser, M., Heining, M., Schmidt, J., Becker, A., Garbe, D., Buchholz, R., Brück, T., 2016. Application of light-emitting diodes (LEDs) in cultivation of phototrophic microalgae: current state and perspectives. *Appl. Microbiol. Biotechnol.* 100, 1077–1088.
- Hogewoning, S.W., Trouwborst, G., Harbinson, J., Van Ieperen, W., 2010. Light distribution in leaf chambers and its consequences for photosynthesis measurements. *Photosynthetica* 48, 219–226.
- Hootsmans, M.J.M., Vermaat, J.E., 1994. Light-response curves of *Potamogeton pectinatus* L. as function of plant age and irradiance level during growth. In: Vierrsen, W.v., Hootsmans, M., Vermaat, J. (Eds.), *Lake Veluwe, a Macrophyte-Dominated System under Eutrophication Stress*. Springer Netherlands, The Netherlands.
- Huner, N.P.A., Bode, R., Dahal, K., Hollis, L., Rosso, D., Krol, M., Ivanov, A.G., 2012. Chloroplast redox imbalance governs phenotypic plasticity: the "grand design of photosynthesis" revisited. *Front. Plant Sci.* 3.
- Jassby, A.D., Platt, T., 1976. Mathematical formulation of relationship between photosynthesis and light for phytoplankton. *Limnol. Oceanogr.* 21, 540–547.
- Kahara, S.N., Vermaat, J.E., 2003. The effect of alkalinity on photosynthesis-light curves and inorganic carbon extraction capacity of freshwater macrophytes. *Aquat. Bot.* 75, 217–227.
- Kalf, J., 2002. *The Phytoplankton, Limnology: Inland Water Ecosystems*. Prentice Hall, p. 40.
- Kirsten, W., Peter, H., 1998. The Photosynthetic Light Dispensation System: application to microphytobenthic primary production measurements. *Mar. Ecol. Prog. Ser.* 166, 63–71.
- Lichtenberg, M., Kuhl, M., 2015. Pronounced gradients of light, photosynthesis and O₂ consumption in the tissue of the brown alga *Fucus serratus*. *New Phytol.* 207, 559–569.
- Madsen, T.V., Sand-Jensen, K., Beer, S., 1993. Comparison of photosynthetic performance and carboxylation capacity in a range of aquatic macrophytes of different growth forms. *Aquat. Bot.* 44, 373–384.
- Masojidek, J., Grobelaar, J.U., Pechar, L., Kobližek, M., 2001. Photosystem II electron transport rates and oxygen production in natural waterblooms of freshwater cyanobacteria during a diel cycle. *J. Plankton Res.* 23, 57–66.
- Menendez, M., Sanchez, A., 1998. Seasonal variations in P-I responses of *Chara hispida* L. and *Potamogeton pectinatus* L. from stream mediterranean ponds. *Aquat. Bot.* 61, 1–15.
- Moejes, F.W., Matuszyska, A., Adhikari, K., Bassi, R., Cariti, F., Cogne, G., Dikaos, I., Falcatore, A., Finazzi, G., Flori, S., Goldschmidt-Clermont, M., Magni, S., Maguire, J., Le Monnier, A., Muller, K., Poolman, M., Singh, D., Spelberg, S., Stella, G.R., Succurro, A., Taddei, L., Urbain, B., Villanova, V., Zabke, C., Ebenhoeh, O., 2017. A systems-wide understanding of photosynthetic acclimation in algae and higher plants. *J. Exp. Bot.* 68, 2667–2681.
- Necchi Jr., O., Zucchi, M.R., 2001. Photosynthetic performance of freshwater Rhodophyta in response to temperature, irradiance, pH and diurnal rhythm. *Phycol. Res.* 49, 305–318.
- Necchi, O., 2004. Light-related photosynthetic characteristics of lotic macroalgae. *Hydrobiologia* 525, 139–155.
- Nielsen, S.L., Sand-Jensen, K., 1989. Regulation of photosynthetic rates of submerged rooted macrophytes. *Oecologia* 81, 364–368.
- Pedersen, O., Colmer, T., Sand-Jensen, K., 2013. Underwater photosynthesis of submerged plants – recent advances and methods. *Front. Plant Sci.* 4, 140.
- Phooprong, S., Ogawa, H., Hayashizaki, K., 2008. Photosynthetic and respiratory responses of *Gracilaria vermiculophylla* (ohmi) papenfuss collected from Kumamoto, Shizuoka and Iwate, Japan. *J. Appl. Phycol.* 20, 743–750.
- Piepho, M., 2017. Assessing maximum depth distribution, vegetated area, and production of submerged macrophytes in shallow, turbid coastal lagoons of the southern Baltic Sea. *Hydrobiologia* 794, 303–316.
- Pilon, J., Santamaria, L., 2002. Clonal variation in morphological and physiological responses to irradiance and photoperiod for the aquatic angiosperm *Potamogeton pectinatus*. *J. Ecol.* 90, 859–870.
- Samuilov, V.D., Fedorenko, T.A., 1999. Lag phase of CO₂-dependent O₂ evolution by illuminated *Anabaena variabilis* cells. *Biochemistry* 64, 610–619.
- Schutter, M., van der Ven, R.M., Janse, M., Verreth, J.A.J., Wijffels, R.H., Osinga, R., 2012. Light intensity, photoperiod duration, daily light flux and coral growth of *Galaxea fascicularis* in an aquarium setting: a matter of photons? *J. Mar. Biol. Assoc. U. K.* 92, 703–712.
- Shafer, D.J., Kaldy, J.E., Sherman, T.D., Marko, K.M., 2011. Effects of salinity on photosynthesis and respiration of the seagrass *Zostera japonica*: a comparison of two established populations in North America. *Aquat. Bot.* 95, 214–220.
- Sorrell, B.K., Dromgoole, F.I., 1986. Errors in measurements of aquatic macrophyte Gas-exchange due to oxygen storage in internal airspaces. *Aquat. Bot.* 24, 103–114.
- Sorrell, B.K., Hawes, I., Schwarz, A.-M., Sutherland, D., 2001. Inter-specific differences in photosynthetic carbon uptake, photosynthate partitioning and extracellular organic carbon release by deep-water characean algae. *Freshw. Biol.* 46, 453–464.
- Thestrup, B., Dam-Hansen, C., Lund, J.B., Rosenqvist, E., 2008. High-power LED illumination system for photosynthetic research on potted plant canopies. In: *Light-Emitting Diodes: Research, Manufacturing, and Application* XII.
- Titus, J.E., Adams, M.S., 1979. Coexistence and the comparative light relations of the Submersed macrophytes *Myriophyllum spicatum* L. and *Vallisneria spiralis* L. *Oecologia* 40, 273–286.
- Walters, R.G., 2005. Towards an understanding of photosynthetic acclimation. *J. Exp. Bot.* 56, 435–447.
- Yano, A., Fujiwara, K., 2012. Plant lighting system with five wavelength-band light-emitting diodes providing photon flux density and mixing ratio control. *Plant Methods* 8, 46.